

Transition-Metal Complexes of Dithiooxamide Ligands. Vibrational Fine Structure in the Electronic Spectra of Symmetrically N,N' -Disubstituted Dithiooxamides and Their Divalent Nickel Ion Complexes

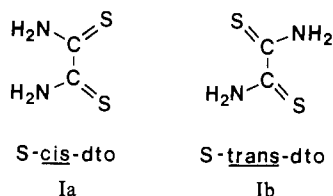
Michael R. Green, Nusrallah Jubran, Bruce E. Bursten,*¹ and Daryle H. Busch*

Received December 5, 1986

UV-vis spectroscopic studies of symmetrically N,N' -disubstituted dithiooxamides, HRNC(=S)C(=S)NRH (N,N' - R_2dto ; $\text{R} = \text{H, Me, Et, } n\text{-Bu, } sec\text{-Bu, benzyl, } p\text{-chlorobenzyl, } o\text{-chlorobenzyl, triphenylmethyl, trimethylsilyl}$), have shown that the electronic spectrum of the dto moiety consists of two transitions, a weak broad $n \rightarrow \pi^*$ transition occurring in the visible region and an intense $\pi \rightarrow \pi^*$ transition in the UV region. A Fenske-Hall approximate molecular orbital calculation on dto suggests the assignment of these transitions as ${}^1\text{A}_g \leftarrow {}^1\text{A}_g$ ($13a_g \rightarrow 4a_g$) and ${}^1\text{B}_u \leftarrow {}^1\text{A}_g$ ($3b_u \rightarrow 4a_u$), respectively. In agreement with additional calculations, N,N' -dialkyl of the dto moiety has been shown to cause a blue shift of the transitions, while N,N' -disilylation has been shown to cause a red shift. The $n \rightarrow \pi^*$ transition of N,N' -Bzl₂dto, which is representative of all of the N,N' -disubstituted dithiooxamides examined, exhibits vibrational fine structure, which resolves greatly upon temperature reduction. The major vibrational progression for N,N' -Bzl₂dto appears to involve the C-C stretch and has a frequency of ca. 1150 cm^{-1} . The UV-vis spectrum of $\text{Ni}(N,N'$ -Bzl₂dto)₂Br₂, which is representative of the group VIII (group 10)[†] divalent metal ion complexes of dithiooxamides formulated as $\text{M}(N,N'$ - $\text{R}_2\text{dto})_2\text{X}_2$, consists of a series of bands in the visible region of varying intensity and an intense band in the UV region. A Fenske-Hall calculation on $\text{Ni}(\text{dto})_2^{2+}$ suggests that the bands in the visible region are due to $\text{M}(d) \rightarrow \text{L} \pi^*$ transitions, while the band in the UV region is due to a $\text{L} \pi \rightarrow \text{L} \pi^*$ transition. Variable-temperature spectral studies of the bands in the visible region suggest that these bands are part of a vibrational progression that is very similar to the major vibrational progression observed for the $n \rightarrow \pi^*$ transition of the free ligand.

Introduction

The discovery of dithiooxamide, $\text{H}_2\text{NC(=S)C(=S)NH}_2$ (I), more than a century ago² marked the birth of a novel and exotic ligand family. The unique chemical properties of dithiooxamides



were not fully recognized by the chemical industry until the late 1940s, but since that time an extraordinarily wide range of applications have been reported in the literature. They have been claimed to be effective metal deactivators in petroleum products,³ to inhibit the action of certain bacteria⁴ and dehydrogenases,⁵ to serve as reagents in the syntheses of histological agents,⁶ and to act as vulcanization accelerators,⁷ as color sources in duplicating processes,^{8,9} and as molecularly oriented dichroic stains in light-polarizing films.¹⁰ Perhaps the most familiar application of dithiooxamides is their use as reagents for the detection¹¹ and determination¹² of various metals. This surprising versatility of the dithiooxamide ligand family has caused a considerable research effort to be directed toward the synthesis of new ligands.¹³ Recently, we have had notable success in developing synthetic methods for the isolation of new ligands.¹⁴

Much of the attention that dithiooxamides have received in the chemical literature, however, has been focused on their transition-metal complexes,¹⁵ particularly their intensely colored polymeric, $[(\text{ML})_n]$,¹⁶ and monomeric, $\text{M}(\text{LH}_2)_2\text{X}_2$,¹⁷ complexes ($\text{M} = \text{Ni, Pd, Pt}$; $\text{LH}_2 =$ dithiooxamide family ligand; $\text{X} =$ halide). Although a thorough study of the infrared spectra for the ligands¹⁸ and the $\text{M}(\text{LH}_2)_2\text{X}_2$ complexes¹⁹ has already been performed, the electronic spectra for these species have not yet been studied in detail. Initial reports on the electronic spectra have appeared for both the free ligands²⁰ and the $\text{M}(\text{LH}_2)_2\text{X}_2$ complexes.^{17b,19a,21} Attempts to interpret the electronic spectral data have led to two

different assignments of the spectral bands in the $\text{M}(\text{LH}_2)_2\text{X}_2$ complexes.^{21a,c} Inasmuch as there is a difference of opinion

- (1) Camille and Henry Dreyfus Foundation Teacher-Scholar, 1984-1989, and Fellow of the Alfred P. Sloan Foundation, 1985-1987.
- (2) Gay-Lussac, M. *Ann. Chim. (Paris)* **1815**, *95*, 136-232.
- (3) Watson, R. W.; Loane, C. M. U.S. Patent 2 484 257, 1949.
- (4) (a) Liebermeister, K. Z. *Naturforsch., B: Anorg. Chem., Org. Chem., Biochem., Biophys., Biol.* **1950**, *5B*, 79-86. (b) Liebermeister, K.; Hageloch, G. Z. *Naturforsch., B: Anorg. Chem., Org. Chem., Biochem., Biophys., Biol.* **1951**, *6B*, 147-155.
- (5) Miller, J. G.; Brody, T. M. *J. Pharmacol. Exp. Ther.* **1957**, *121*, 43-54.
- (6) (a) Karrer, P.; Sanz, H. C. *Helv. Chim. Acta* **1944**, *27*, 619-621. (b) Karrer, P.; Sanz, H. C. Swiss Patent 238 517, 1945. (c) Karrer, P.; Leiser, P.; Graf, W. *Helv. Chim. Acta* **1944**, *27*, 624-625.
- (7) Naylor, R. A.; Hook, E. O. U.S. Patent 2 723 969, 1955.
- (8) (a) Miller, C. S.; Clark, B. L. U.S. Patent 2 663 656, 1953. (b) Ostile, Dean A. U.S. Patent 3 481 759, 1969; *Chem. Abstr.* **1969**, *71*, 72167. (c) Yarian, Dean R. U.S. Patent 4 334 015, 1982; *Chem. Abstr.* **1982**, *97*, 101744. (d) Fraser, William J. U.S. Patent 4 244 604, 1981; *Chem. Abstr.* **1981**, *94*, 165742. (e) Haas, Howard C. U.S. Patent 3 287 154, 1966; *Chem. Abstr.* **1967**, *66*, 47524.
- (9) Ditto, Inc. British Patent 802 170, 1958.
- (10) Amon, W. F., Jr.; Kane, M. W. U.S. Patent 2 505 085, 1950.
- (11) Feigel, F. *Spot Tests*, 4th ed.; translated by R. E. Oesper; Elsevier: New York, 1954; Vol. 1, pp 83, 139, 145.
- (12) (a) Pheline, J. M.; Castro, R. *Congr. Group. Av. Methodes. Anal. Spectrogr. Prod. Metall.* **1947**, *8*, 47, 177. (b) Tananaev, I. V.; Levitman, S. Y. *Zh. Anal. Khim.* **1949**, *4*, 212. (c) Vaecq, S. V. *Anal. Chim. Acta* **1954**, *10*, 48-67. (d) Welcher, F. J. *Organic Analytical Reagents*; Van Nostrand: New York, 1948; p 148.
- (13) (a) Woodburn, H. M.; Scroog, C. E. *J. Org. Chem.* **1952**, *17*, 371-378. (b) Woodburn, H. M.; Platek, W.; Graminiski, E. L. *J. Org. Chem.* **1958**, *23*, 319-320. (c) Hurd, R. H.; DeLaMater, G.; McElheny, G. C.; Turner, R. J.; Wallingford, V. H. *J. Org. Chem.* **1961**, *26*, 3980-3987. (d) Hurd, R. H.; DeLaMater, G.; McDermott, J. P. *J. Org. Chem.* **1961**, *27*, 269-272. (e) Walter, W.; Luke, H. W.; Voss, Jürgen *Justus Liebig's Ann. Chem.* **1975**, 1808-1821.
- (14) Jubran, N.; Davis, W. M.; Green, M. R.; Bursten, B. E.; Busch, D. H., submitted for publication.
- (15) See, for example: (a) Hurd, R. H.; DeLaMater, G.; McElheny, G. C.; McDermott, J. P. In *Advances in the Chemistry of Coordination Compounds*; Kischner, S., Ed.; MacMillan: New York, 1961. (b) Hurd, R. N.; DeLaMater, G. *Chem. Rev.* **1961**, *61*, 45-86.
- (16) See, for example: (a) Menabus, L.; Pellacani, G. C.; Peyronel, G. *Inorg. Nucl. Chem. Lett.* **1974**, *10*, 187-191. (b) Hurd, R. N.; DeLaMater, G. C.; McElheny, G. C.; Peiffer, L. V. *J. Am. Chem. Soc.* **1960**, *82*, 4454-4458.
- (17) See, for example: (a) Pignedoli, A.; Peyronel, G. *Gazz. Chim. Ital.* **1963**, *93*, 564-569. (b) Peyronel, G.; Pellacani, G. C.; Pignedoli, A. *Inorg. Chim. Acta* **1971**, *5*, 627-633. (c) Peyronel, G.; Fabretti, A. C.; Pellacani, G. C. *J. Inorg. Nucl. Chem.* **1973**, *35*, 973-977. (d) Peyronel, G.; Pellacani, G. C. *Inorg. Chim. Acta* **1974**, *9*, 189-192.

[†] The periodic group notation in parentheses is in accord with recent actions by IUPAC and ACS nomenclature committees. A and B notation is eliminated because of wide confusion. Groups IA and IIA become groups 1 and 2. The d-transition elements comprise groups 3 through 12, and the p-block elements comprise groups 13 through 18.

Table I. Electronic Spectral Data for Symmetrically N,N'-Disubstituted Dithiooxamides^a

ligand RHNC(=S)C(=S)NHR	$\pi \rightarrow \pi^*$ λ_{\max} , nm ($10^{-4}\epsilon$, M ⁻¹ cm ⁻¹)	$n \rightarrow \pi^*$ λ_{\max} , nm (ϵ , M ⁻¹ cm ⁻¹)
R = H	311.5 (1.0)	479 (18), 500 (18), 540 (sh) ^b
R = Me	296 (1.3)	435 (18), 456 (17), 480 (sh)
R = Et	303.5 (1.3)	452 (28), 480 (sh), 520 (sh)
R = <i>n</i> -Bu	304 (1.5)	440 (25), 458 (23), 480 (sh)
R = <i>sec</i> -Bu	304.5 (1.3)	438 (17), 458 (17), 480 (sh)
R = benzyl ^c	308 (1.1)	444 (29), 462 (30), 492 (sh)
R = <i>p</i> -chlorobenzyl ^c	307 (1.4)	447 (31), 462 (31), 492 (sh)
R = <i>o</i> -chlorobenzyl ^c	306.5 (1.4)	444 (32), 460 (32), 488 (sh)
R = triphenylmethyl ^{c,d}	307 (0.8), 266 (0.7), 260 (0.7)	480 (27), 505 (28), 540 (sh)
R = trimethylsilyl ^{d,f}	317	460, 488, 516, 548, 592

^aSpectra were recorded on a Varian 2300 spectrophotometer in absolute ethanol unless otherwise noted. ^bsh = shoulder. ^cSolvent = methylene chloride. ^dSee text for more detail. ^eSolvent = hexane. ^fMolar absorptivity value not determined.

concerning the electronic structure of the group VIII (group 10)[†] metal complexes of dithiooxamides, and given our interest in the spectroscopic properties of these systems, we have undertaken a combined experimental and theoretical investigation of the electronic structure and bonding of the complexes. In this paper we will show a great self-consistency between our calculational and spectroscopic results, leading to the conclusion that *neither* of the previously advanced assignments is entirely correct. In addition, we report low-temperature spectroscopic studies of both the free ligands and their divalent nickel ion complexes, which show that vibrational fine structure plays an important and heretofore unreported role in the electronic spectroscopy of these species.

Experimental Section

Sample Preparation. Dithiooxamide was purchased from Aldrich Chemical Co. and was recrystallized from a hot ethanolic solution containing activated charcoal. The symmetrically N,N'-disubstituted dithiooxamides, RHNC(=S)C(=S)NHR, listed in Table I were prepared and characterized according to literature methods. The procedure from ref 13a was followed for R = Me and Et; that from ref 13b for R = *n*-Bu; that from ref 13c for R = *sec*-Bu, benzyl, *p*-chlorobenzyl, and *o*-chlorobenzyl; that from ref 13d for R = triphenylmethyl; and that from ref 13e for R = trimethylsilyl. Ni(*N,N'*-Bzl₂dto)₂Br₂ (*N,N'*-Bzl₂dto = *N,N'*-dibenzyl(dithiooxamide) was prepared and characterized according to the procedure given in ref 21a.

Electronic Spectra. The electronic spectra for the ligands listed in Table I were recorded on a Varian 2300 spectrophotometer. The concentrations employed were 2.0×10^{-2} M in the 800–400-nm range and 4.0×10^{-5} M in the 400–200-nm range. For *N,N'*-bis(triphenylmethyl)dithiooxamide and *N,N'*-bis(trimethylsilyl)dithiooxamide the spectra were recorded in methylene chloride and hexane, respectively. The remainder of the ligands were examined in absolute ethanol. The EPA used in the low-temperature experiments was prepared by mixing anhydrous diethyl ether, freshly distilled isopentane, and absolute ethanol in a 5:5:2 volume ratio and was stored over molecular sieves until used. Crystals of *N,N'*-dibenzyl(dithiooxamide) were grown by slow evaporation from a benzene solution. The KBr pellets for Ni(*N,N'*-Bzl₂dto)₂Br₂ and *N,N'*-Bzl₂dto were made by grinding each compound with oven-dried KBr and then transferring each mixture to a standard hydraulic press. No evidence of decomposition was noted during sample preparation and spectral recording.

The variable-temperature spectra were recorded on a Cary 17D spectrophotometer, which was interfaced to an Apple II Plus computer using an interface package supplied by Varian. Low temperatures were achieved by using a Janis Research Co. detachable tail research Dewar

flask (cryostat). Temperature was determined and controlled to 0.1 K with a Lake Shore Cryotronics Model DRC-80C digital cryogenic thermometer/controller. Data were collected by using a modified version of the Cary 17D/Apple II data management system.²²

Results and Discussion

The electronic spectra for several dithiooxamide ligands²⁰ and their M(LH₂)₂X₂ complexes^{17b,19a,21} have been reported in the literature, and assignments of the observed spectra have been suggested. The assignment of the free-ligand spectra was straightforward and consequently has not been disputed in the literature. As will be detailed below, the electronic spectra for several symmetrically N,N'-disubstituted dithiooxamides exhibited vibrational fine structure. Surprisingly, this vibrational fine structure has not been previously reported, even though it is discernible at room temperature. In contrast to the free ligands, a simple assignment of the M(LH₂)₂X₂ spectra was not apparent. Currently two interpretations for the spectral data have been suggested,^{21a,c} and the differences are due, in part, to a lack of structural data for the M(LH₂)₂X₂ complexes. In the course of our study we noticed a great similarity between the pattern of bands exhibited by the M(LH₂)₂X₂ complexes and the pattern of vibrational bands exhibited by the free ligands. This suggested to us that the band pattern observed for the M(LH₂)₂X₂ complexes was actually due to vibrational fine structure. To further explore this possibility, we initiated an investigation into the electronic structures and spectra of the ligands (section I below) and their M(LH₂)₂X₂ complexes (section II below). While a brief report on the electronic structure of the ligands has been published,²⁰ no studies of the electronic structure of the M(LH₂)₂X₂ complexes have been reported. In view of this we have performed Fenske-Hall molecular orbital calculations²³ on several ligands and their Ni(LH₂)₂²⁺ complexes.²⁴ The calculational results in conjunction with low-temperature electronic spectral measurements indicate a need to reassign the transitions observed in the M(LH₂)X₂ spectra.

I. Dithiooxamide Ligands. The electronic spectrum of dithiooxamide (dto) in absolute ethanol at room temperature has been reported previously.²⁰ The spectrum is characterized by two transitions: a broad, structured band centered at ca. 490 nm ($\epsilon \approx 20$) and a much more intense absorption centered at ca. 310 nm ($\epsilon \approx 1.0 \times 10^4$). The assignment of these transitions is readily apparent from a consideration of the molecular orbitals of dithiooxamide. A molecular orbital diagram for the valence region of *S-trans*-dto under C_{2h} symmetry is shown in Figure 1.²⁴ The highest occupied molecular orbital (HOMO) of the molecule, the 13a_g, is a lone-pair orbital that consists almost entirely (94%) of contributions from the in-plane S 3p orbitals that are perpendicular to the C–S bonds. This orbital will be of great importance in the binding of dto to a metal center, as will be discussed later. The lowest unoccupied molecular orbital (LUMO), the 4a_u, is part of the π system of the molecule and is delocalized throughout the

- (18) See, for example: (a) Desseyne, H. O.; Van der Veken, B. J.; Aarts, A. *Can. J. Spectrosc.* **1977**, *22*, 84–87. (b) Desseyne, H. O.; Van der Veken, B. J.; Herman, M. A. *Appl. Spectrosc.* **1978**, *32*, 101–105. (c) Desseyne, H. O.; Aarts, A. J.; Esmans, E.; Herman, M. A. *Spectrochim. Acta, Part A* **1979**, *35A*, 1203–1211.
- (19) See, for example: (a) Hofmans, H.; Desseyne, H. O.; Dommissee, R.; Herman, M. A. *Bull. Soc. Chim. Belg.* **1982**, *91*, 175–188. (b) Hofmans, H.; Desseyne, H. O.; Herman, M. A. *Spectrochim. Acta Part A* **1982**, *38A*, 1307–1318.
- (20) Persson, B.; Sandström, J. *Acta Chem. Scand.* **1964**, *18*, 1059–1077.
- (21) (a) Peyronel, G.; Pellacani, G. C. *Inorg. Nucl. Chem. Lett.* **1972**, *8*, 299–303. (b) Aarts, A. J.; Desseyne, H. O.; Herman, M. A. *Inorg. Chim. Acta* **1978**, *29*, L197–L198. (c) Hofmans, H.; Desseyne, H. O. *Bull. Soc. Chim. Belg.* **1986**, *95*, 83–88.

(22) Braydich, M. Ph.D. Thesis, The Ohio State University, 1987.

(23) Hall, M. B.; Fenske, R. F. *Inorg. Chem.* **1972**, *11*, 768–775.

(24) A full account of the details of the calculation will appear in a subsequent paper.

C (39%), S (39%), and N (22%) p_π orbitals. This orbital is C–N and C–S antibonding but is bonding between the carbon atoms. The lowest energy electronic transition of the molecule is predicted to be the transfer of an electron from the HOMO to the LUMO, i.e. the $n \rightarrow \pi^*$ transition $13a_g \rightarrow 4a_u$ (${}^1A_u \leftarrow {}^1A_g$). This transition is symmetry allowed but is expected to be weak due to the mutual orthogonality of the AO's comprising the $13a_g$ and the $4a_u$ MO's. The assignment of the first band as $n \rightarrow \pi^*$ agrees with the previous assignment of the electronic spectrum of *dto*.²⁰ The intense UV absorption at $\lambda_{\max} = 311.5$ nm is also predicted to involve the transfer of an electron to the LUMO, this time from the occupied $3b_g$ orbital. The $3b_g$, like the LUMO, is part of the π system of the molecule, consisting of 81% S, 13% N, and 6% C p_x contributions. The orbital is C–S bonding and C–N and C–C antibonding. Thus, in agreement with the earlier study,²⁰ the second band is assigned to an allowed $\pi \rightarrow \pi^*$ transition, the $3b_g \rightarrow 4a_u$ (${}^1B_g \leftarrow {}^1A_g$), and is expected to be much more intense than the $n \rightarrow \pi^*$ transition.

Generally, it is observed (Table I) that symmetrical N,N' -dialkylation of the *dto* moiety leads to a blue shift and an increase in the intensity of both the $n \rightarrow \pi^*$ and $\pi \rightarrow \pi^*$ transitions.²⁵ The blue shift of the transitions is consistent with the results of a Fenske–Hall calculation on N,N' -Me₂*dto*.

A detailed examination of the visible spectra for the ligands listed in Table I indicates that the $n \rightarrow \pi^*$ transition for each ligand consists of several closely overlapping bands, which appear as shoulders on the $n \rightarrow \pi^*$ transition. Since the calculations did not indicate that additional electronic transitions should occur in this region, we initiated a low-temperature spectroscopic investigation of the $n \rightarrow \pi^*$ transition of these ligands. Our initial studies, comparing the 298 K solution and 100 K glass spectra of the $n \rightarrow \pi^*$ transition of N,N' -diethyldithiooxamide in EPA, showed considerable resolution of the spectral features into an apparent Franck–Condon progression. Attempts to obtain spectra at lower temperatures in this solvent mixture failed, because of the decreased solubility of the ligand.

To eliminate solubility problems we continued our low-temperature investigation of the ligands in the solid state using crystals of the ligands. Figure 2 shows a comparison of the 298 K, 100 K, and 5 K crystal spectra for N,N' -dibenzoyldithiooxamide. In contrast to the broad band observed in the 298 K solution spectrum, the 298 K crystal spectrum is separated into four well-resolved peaks and a shoulder at ca. 24 250 cm^{-1} . The spacing between these bands, although not uniform, is on the order of 1300 cm^{-1} . Lowering the temperature to 100 K sharpens each band considerably, and additional fine structure begins to appear on several of the major bands. Reduction of the temperature to 5 K dramatically increases the resolution of the spectrum; over 70 peaks are present in this narrow spectral region. We believe that the presence and temperature dependence of this structure are incontrovertible evidence that it is due to vibrational modes coupled to the electronic transition and suggest that coupled vibrational fine structure plays a significant role in the spectroscopy of these ligands. The pattern of the bands and the energetic spacing

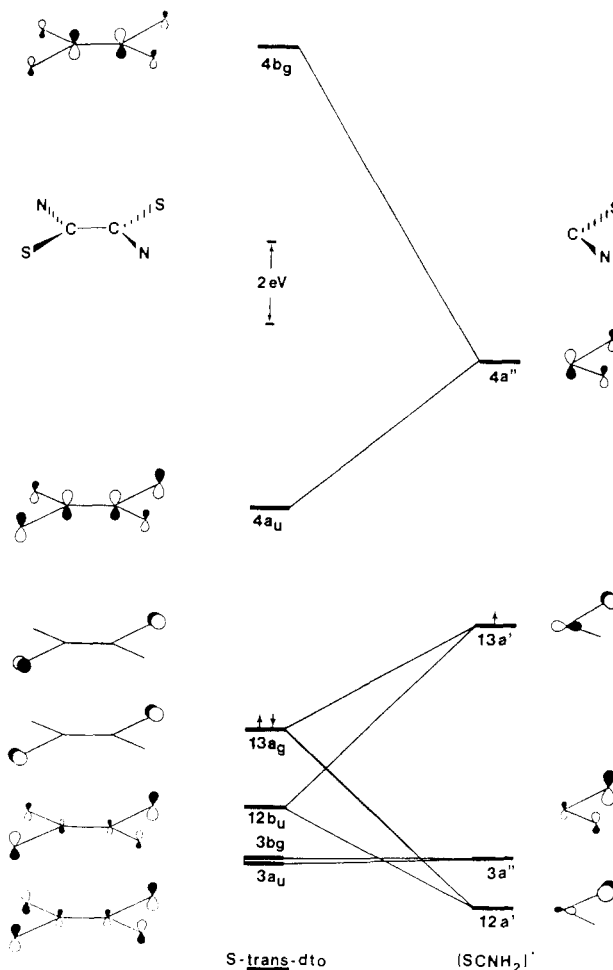


Figure 1. Molecular orbital diagram for the valence region of dithiooxamide.

between them signify that more than one vibrational progression is present in the observed spectrum.

Despite its "noisy" appearance, the spectrum at 5 K is quite reproducible. A preliminary analysis of the spectral data indicates that at least three unique vibrational frequencies are contributing to the spectrum. Two of the modes are of low energy, one ca. 52 cm^{-1} , ν_1 , and the other ca. 180 cm^{-1} , ν_2 . Their low energy suggests that they may be crystal lattice modes.²⁷ The ν_1 mode is responsible for the structure of the band centered at 18 800 cm^{-1} , which appears to be the 0–0 band of the major vibrational progression. An enlargement of this region of the spectrum is shown in the inset in Figure 2. The ν_2 mode appears mainly in combination bands with the ν_1 mode and accounts for the transitions occurring in the 19 000–19 800 cm^{-1} region. The third mode, ν_3 , is the major vibrational progression and has a frequency of ca. 1150 cm^{-1} . Since low-temperature electronic spectroscopy measures vibrational frequencies characteristic of the excited electronic state of the molecule, a correct assignment of ν_3 necessitates that the bonding characteristics of the orbitals involved be considered. As stated above, the $4a_u$ π^* orbital is the acceptor orbital in the $n \rightarrow \pi^*$ transition. This orbital is carbon–carbon bonding but carbon–nitrogen and carbon–sulfur antibonding (Figure 1). If ν_3 were primarily based on the excited-state C–C stretch, one would expect its frequency to be larger than the ground-state frequency of the C–C stretch (849 cm^{-1} for *dto*^{18a}). If ν_3 were primarily based on the C–N or C–S stretch, however, its frequency would be expected to decrease from the respective C–N or C–S ground-state stretching frequencies, which, for *dto*, are 1440 and 832 cm^{-1} , respectively.^{18a} Since ν_3 has a frequency of ca. 1150 cm^{-1} , this implies that either the C–C or C–N stretch is the active

(25) Two of the ligands presented in Table I exhibit features that require additional discussion. For N,N' -bis(triphenylmethyl)dithiooxamide three bands occur in the UV region of the spectrum in contrast to one band for the other N,N' -disubstituted dithiooxamides. The low-energy band at 307 nm is in the same region as the $\pi \rightarrow \pi^*$ transitions for the other symmetrically N,N' -disubstituted dithiooxamides and can be assigned tentatively as the $\pi \rightarrow \pi^*$ transition characteristic of the *dto* moiety. The two higher energy transitions (266 and 260 nm) are in the energy range characteristic of $\pi \rightarrow \pi^*$ transitions in isolated phenyl rings.²⁶ For N,N' -bis(trimethylsilyl)dithiooxamide the $n \rightarrow \pi^*$ and $\pi \rightarrow \pi^*$ bands exhibit a red shift relative to *dto*. Molecular orbital calculations on the model molecule, N,N' -disilyldithiooxamide, indicate that the silyl group decreases the charge on the nitrogen atom relative to the methyl group in N,N' -dimethyldithiooxamide. This leads to a change in the percent character composition for the π system of dithiooxamide and results in an increased localization of the π and π^* orbitals on sulfur and carbon, consequently decreasing the energetic spacing between the orbitals involved in the transitions.²⁴

(26) Bassler, G. C.; Morrill, T. C.; Silverstein, R. M. *Spectrometric Identification of Organic Compounds*; Wiley: New York, 1981; Chapter 6.

(27) Hitchman, M. A.; Cassidy, P. J. *Inorg. Chem.* **1979**, *18*, 1745–1754.

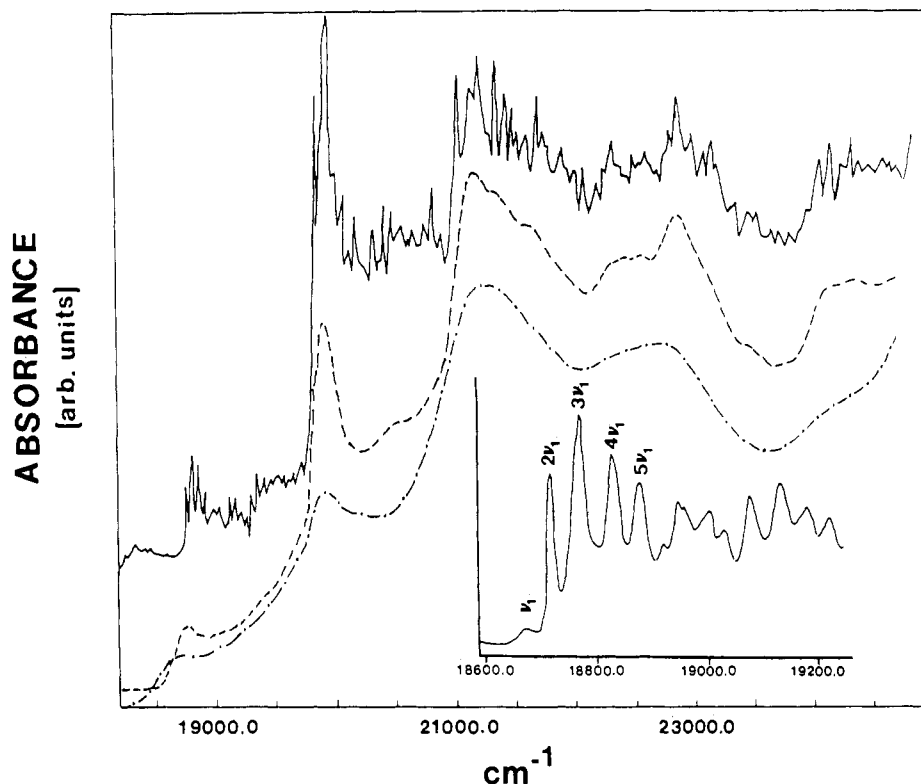
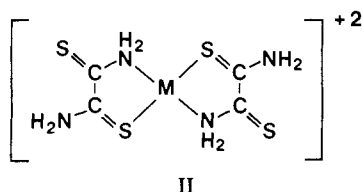


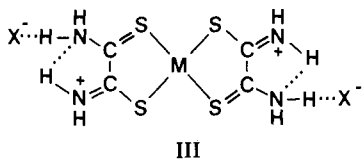
Figure 2. Variable-temperature crystal spectra for the $n \rightarrow \pi^*$ transition of N,N' -dibenzylidithiooxamide at (a) 298 K (---), (b) 100 K (---), and (c) 5 K (—). Inset: Enlargement of initial vibrational progression.

vibration. The C–C and C–N stretching frequencies for the N,N' -dialkyldithiooxamides are generally higher than that of dto itself,^{18c} suggesting that the active vibration is the C–C stretch. Studies are currently in progress to confirm the assignment of the major vibrational progression and to more thoroughly analyze the abundance of vibrational fine structure data present in dithiooxamide ligands.²⁸

II. $M(LH_2)_2X_2$ Complexes. The coordination mode of dithiooxamide ligands in their $M(LH_2)_2X_2$ complexes perplexed investigators for many years. It was originally thought that the metal was S, N coordinated by each dithiooxamide ligand, yielding a square-planar complex of nearly C_{2h} symmetry (II).^{18b,21a,29} In



contrast, it is now believed that each ligand acts as a bidentate sulfur chelating ligand, yielding a square-planar complex of nearly D_{2h} symmetry (III).^{22c,30} As shown by III, it has been suggested



that the halide ligands do not occupy axial positions in the com-

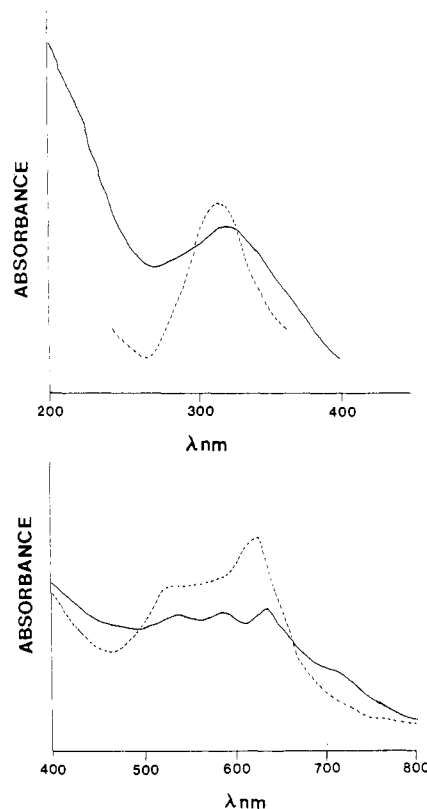


Figure 3. Comparative UV-vis spectra of $Ni(N,N'$ -Bzl₂dto)₂Br₂ (a) in methylene chloride (---) ($800\text{--}400\text{ nm}$, $1.0 \times 10^{-4}\text{ M}$; $360\text{--}240\text{ nm}$, $1.0 \times 10^{-5}\text{ M}$) and (b) in a KBr pellet (—).

(28) Bursten, B. E.; Busch, D. H.; Green, M. R.; Jubran, N., unpublished results.

(29) See, for example: (a) Claser, G.; Pellacani, C.; Memabue, L.; Peyronel, G. *Gazz. Chim. Ital.* **1974**, *104*, 1095–1099. (b) Fabretti, A. C.; Rellacani, G. C.; Peyronel, G. *J. Inorg. Nucl. Chem.* **1976**, *38*, 443–445.

(30) Bursten, B. E.; Busch, D. H.; Green, M. R.; Jubran, N., unpublished results.

plexes but rather form hydrogen bonds with the thioamide hydrogen atoms.¹⁹ If dto is to achieve this S-cis coordination geometry, the ligand must rotate about the central C–C bond to change from the S-trans geometry of the free ligand. Fenske–Hall calculations show that this structural rearrangement does not greatly affect the electronic structure of the ligand. Like that

of *S-trans*-dto, the HOMO for *S-cis*-dto is also a sulfur lone-pair orbital. This orbital, the $12b_1$, is a linear combination of in-plane S 3p atomic orbitals (98%) directed perpendicular to the C–S bonds. The LUMO for *S-cis*-dto, the $4b_2$, possesses the same bonding characteristics as the LUMO for *S-trans*-dto, the $4a_u$, and the two orbitals are nearly identical in composition. The relevant occupied π orbitals for each geometry, the *S-trans* $3b_g$ and the *S-cis* $3a_2$, are similarly isomorphous.

The electronic spectrum for $\text{Ni}(\text{N},\text{N}'\text{-Bzl}_2\text{dto})_2\text{Br}_2$ ($\text{N},\text{N}'\text{-Bzl}_2\text{dto} = \text{N},\text{N}'\text{-dibenzylidithiooxamide}$) in methylene chloride at room temperature is shown in Figure 3a. The spectrum is characterized by two overlapping bands in the visible region and an intense broad band in the UV region. The broad band in the UV region is centered at 315 nm and has a molar absorptivity value of 5.0×10^4 . The bands occurring in the visible region have λ_{max} values of 618 and 540 nm with molar absorptivity values of 3.40×10^3 and 2.35×10^3 , respectively. Figure 3b shows a room-temperature KBr spectrum of $\text{Ni}(\text{N},\text{N}'\text{-Bzl}_2\text{dto})_2\text{Br}_2$. In the solid-state spectrum additional bands become apparent. There are now three bands in the visible region with λ_{max} values of 634, 584, and 530 nm. Additionally, a weak shoulder is present at ca. 704 nm. The band in the UV region is broader than it was in solution and is shifted slightly toward lower energy ($\lambda_{\text{max}} = 320$ nm).

As stated earlier, two interpretations of the spectroscopic data of the $\text{M}(\text{LH}_2)_2\text{X}_2$ complexes have been advanced. The earlier interpretation advanced by Peyronel et al. was based on C_{2h} symmetry, considering an S,N coordination of the metal by each ligand.^{17b} For the complexes examined, four bands were reported to occur in the visible region of the spectrum. Of these four the three low-energy bands were assigned as $d \rightarrow d$ transitions, while the highest energy band was assigned to a charge-transfer transition. A later study suggested that the second highest energy band was also charge transfer in nature.^{21a} The more recent interpretation advanced by Desseyn et al. was based on the D_{2h} symmetry that results from a bidentate sulfur chelation of the metal by each ligand.^{21c} At this time, it was recognized that the great intensity of several of the visible bands indicated that charge-transfer transitions dominated this region of the spectrum. In fact, the spectroscopic data reported showed that the intense bands occurring in the 400–600-nm region exhibited spectral shifts for the series of metals nickel, palladium, and platinum similar to the spectral shifts observed by Gray et al.³¹ for the series of $\text{M}(\text{mnt})_2^{2-}$ complexes ($\text{mnt}^{2-} = \text{maleonitriledithiolate}$). The reported energetic ordering for the intense visible bands, which were independent of the ligand and anion, of the $\text{M}(\text{LH}_2)_2\text{X}_2$ complexes was $\text{Ni} \cong \text{Pt} < \text{Pd}$, as was also found for the $\text{M}(\text{mnt})_2^{2-}$ complexes. This similarity in spectral properties leads to the conclusion that the intense transitions were $\text{M}(\text{d}) \rightarrow \text{L} \pi^*$ charge-transfer bands in analogy to the assignment made by Gray et al. for the $\text{M}(\text{mnt})_2^{2-}$ complexes. For the $\text{M}(\text{LH}_2)_2\text{X}_2$ complexes in which the metals were palladium or platinum, weak low-energy bands were observed. These bands were absent for the nickel complexes. These bands are similar to the weak shoulder seen at ca. 704 nm in Figure 3b and were assigned as $d \rightarrow d$ transitions. In the UV region, a broad intense band was observed in the range 328–315 nm for the nickel complexes and at ca. 280 nm for the palladium complexes. This band was not located for the platinum complexes, since it was expected to occur at higher energy and could not be seen due to the absorption of the KX matrix employed. This UV band is similar to the band seen in Figure 3b centered at ca. 320 nm and was assigned as a $\text{L} \sigma \rightarrow \text{M}$ charge-transfer transition. An additional band was observed for the Ni and Pd complexes at ca. 215 nm and was assigned as a $\text{L} \pi \rightarrow \text{L} \pi^*$ transition. We feel that the position of this "band" cannot be considered accurate and that, in fact, this band may not truly exist. The reported spectra were recorded with reference to a blank KX pellet. The cutoff region for KX pellets is ca. 200–210 nm,³² which is very

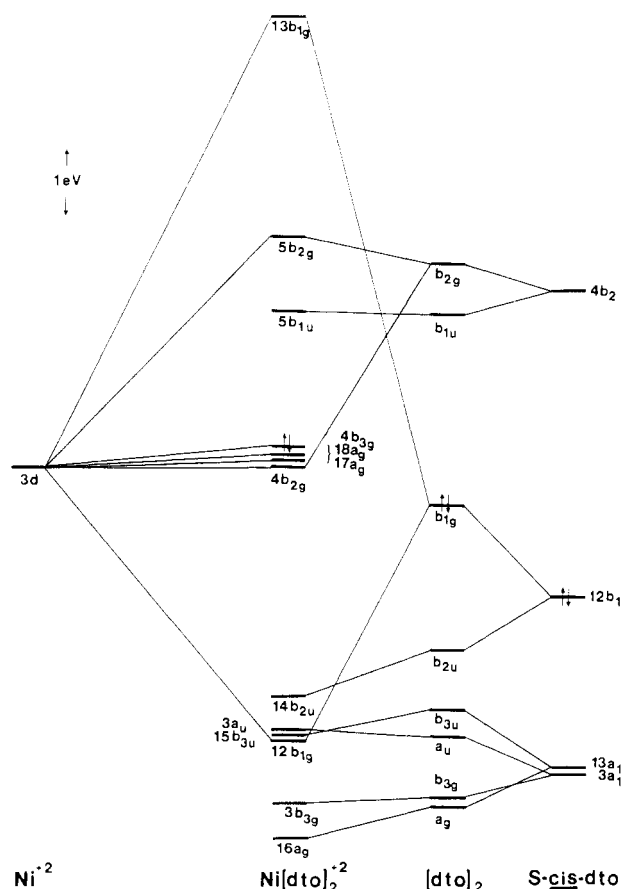


Figure 4. Molecular orbital diagram for $\text{Ni}(\text{dto})_2^{2+}$ showing the interaction of the valence dto group orbitals with the Ni 3d atomic orbitals.

close to the position of this band. Referencing to a blank KX pellet is not the optimal experimental condition and raises concern about the quality of spectral data obtained near the cutoff region. As shown in Figure 3b, our spectral results, which were not referenced to a blank KX pellet, did not show an absorption band at 215 nm but rather a gradual absorption increase leading into the cutoff region. Finally, a weak band was observed for the platinum complexes in the energy range 420–375 nm but was not assigned. The overall energetic sequence of transitions suggested by the authors was $d \rightarrow d < \text{M}(\text{d}) \rightarrow \text{L} \pi^* < \text{L} \sigma \rightarrow \text{M} < \text{L} \pi \rightarrow \pi^*$; however, a Fenske–Hall molecular orbital calculation on $\text{Ni}(\text{dto})_2^{2+}$ as a model for the $\text{M}(\text{LH}_2)_2\text{X}_2$ complexes contradicts this energetic sequence of transitions.

A molecular orbital diagram for the valence region of $\text{Ni}(\text{dto})_2^{2+}$ is shown in Figure 4. The interaction of two *S-cis*-dto ligands with a divalent nickel ion leads to the formation of $\text{Ni}(\text{dto})_2^{2+}$, a complex which is believed to have four Ni–S interactions in an approximately square-planar arrangement.³⁰ The main interaction of *S-cis*-dto with the nickel center is the formation of nickel–sulfur σ -bonding orbitals, through donation primarily from the $12b_1$ HOMO of *S-cis*-dto to the nickel orbitals. Under D_{2h} symmetry the $12b_1$ gives rise to ligand group orbitals (LGO's) of b_{2u} and b_{1g} symmetries. The antisymmetric combination, b_{1g} LGO, is of correct symmetry to interact with the in-plane nickel $3d_{xy}$ orbital, which has lobes directed toward the sulfur atoms. This interaction forms the $12b_{1g}$ Ni(d)–L σ orbital and the $13b_{1g}$ Ni(d)–L σ^* orbital (Figure 4, center). This interaction is quite strong, and extensive mixing between the b_{1g} LGO and the nickel $3d_{xy}$ occurs. A percent character analysis of these orbitals reveals that the $12b_{1g}$ is composed of 35% Ni $3d_{xy}$ and 61% b_{1g} LGO, while the $13b_{1g}$ is 55% Ni $3d_{xy}$ and 40% b_{1g} LGO. Also attesting to the strength of the interaction is a Mulliken population analysis, which shows

(31) (a) Gray, H. B. In *Transition Met. Chem.* (N.Y.) 1965, 1, 239–287. (b) Shupack, S. I.; Billig, E.; Clark, R. J. H.; Williams, R.; Gray, H. B. *J. Am. Chem. Soc.* 1964, 86, 4594–4602. (c) Stiefel, E. I.; Waters, J. H.; Billig, E.; Gray, H. B. *J. Am. Chem. Soc.* 1965, 87, 3016–3017.

(32) Ford, R. A.; Gordon, A. J. *The Chemist's Companion: A Handbook of Practical Data, Techniques, and References*; Wiley: New York, 1972; pp 168, 181.

that the b_{1g} LGO donates 0.87 e to the nickel center. σ donation also occurs from the b_{2u} LGO to the Ni $4p_y$, from the b_{3u} LGO to the Ni $4p_x$, and from the a_g LGO to the Ni $4s$ orbital. The amount of electron density donated from these LGO's to the Ni center (~ 0.2 e each) is much smaller than that donated by the b_{1g} LGO, emphasizing the major role the b_{1g} LGO plays in the σ -bonding network. The interaction of the π system of *S-cis*-dto with the nickel center is quite weak. The only significant π interaction is the donation of 0.15 e from the metal to the b_{2g} LGO, slightly elevating the energy of this orbital.

The end result of the strong σ -bonding interaction and the weak π -bonding interaction is an electronic structure in which the highest occupied molecular orbitals of $Ni(dto)_2^{2+}$ are predominantly metal based, while the lowest unoccupied molecular orbitals are predominantly ligand based ($5b_{1u}$ is 96% b_{1u} LGO, and $5b_{2g}$ is 93% b_{2g} LGO). Due to the presence of the low-lying dto $4b_2 \pi^*$ orbital, the electronic structure found for $Ni(dto)_2^{2+}$ differs from that normally encountered for classical square-planar complexes, such as $[PtCl_4]^{2-}$ and $[Ni(CN)_4]^{2-}$. As a result, the spectral pattern we predict for $Ni(dto)_2^{2+}$ will be different from the spectral pattern exhibited by classical square-planar complexes.

The electronic structure we found for the $M(LH_2)_2^{2+}$ complexes can be readily compared to the tetra-*S*-coordinated square-planar complexes described by Gray et al.³¹ and by Hoffmann et al.³³ Gray et al. have described systems, such as $[Ni(mnt)_2]^{2-}$, in which the energetic ordering of the valence MO's was $L \pi^* > Ni(3d)-L \sigma^* > Ni(3d) \approx L \pi > Ni(3d)-L \sigma$. In contrast, Hoffmann et al. have described systems, such as $[Ni(edt)_2]$ (*edt* = ethylenedithiolate), in which the energetic ordering of the valence MO's was $Ni(3d)-L \sigma^* > L \pi^* > Ni(3d) > L \pi > Ni(3d)-L \sigma$. The calculated energetic ordering of the valence MO's for $Ni(dto)_2^{2+}$ resembles that found in the latter case. The principal difference between the dithiolates that Gray et al. and Hoffmann et al. have discussed and the dithiooxamides discussed here is that the former act as π donors whereas the latter act as moderate π acceptors.

The π -donor vs. π -acceptor ability of a given ligand depends on two factors: (1) the energies of the highest occupied ligand π orbitals and of the lowest unoccupied ligand π^* orbitals relative to the energy of the metal *d* orbitals and (2) the magnitude of the overlaps between the ligand π and π^* orbitals and the metal *d* orbitals. Assuming that the overlaps between the ligand π and π^* orbitals and the metal *d* orbitals do not differ substantially when the three ligands, *dto*, *mnt*²⁻, and *edt*, are compared, the π -donor vs. π -acceptor ability of each ligand will be determined by their relative energies. In $[Ni(mnt)_2]^{2-}$ the *mnt*²⁻ π and π^* orbitals are relatively high in energy compared to the Ni 3*d* orbitals. The *mnt*²⁻ π system is high enough in energy so that upon coordination to the nickel center the π orbitals form the highest occupied molecular orbitals of the complex, while the *mnt*²⁻ π^* orbitals are energetically above the $Ni(3d)-L \sigma^*$ orbital.³³ In $[Ni(edt)_2]$ the *edt* π system is lower in energy than that of *mnt*²⁻. Upon complexation to the nickel center, the *edt* π orbitals are energetically below the nickel 3*d* orbitals and the *edt* π^* orbitals are energetically below the $Ni(3d)-L \sigma^*$ orbital. Their energetic positioning and overlap are such that *edt* functions as a π -donor ligand. In $Ni(dto)_2^{2+}$ the *dto* π system is relatively low in energy compared to the nickel 3*d* orbitals. The occupied *dto* π orbitals are low enough in energy so that they are nonbonding, while the *dto* π^* orbitals are low enough in energy to act as moderate π acceptors, accepting a total of 0.2 e from the divalent nickel ion center.

On the basis of symmetry our model calculation predicts the following symmetry-allowed valence transitions, which are listed in increasing energetic order: four $M(d) \rightarrow L \pi^*$ transitions ($4b_{3g} \rightarrow 5b_{1u}$, $18a_g \rightarrow 5b_{1u}$, $17a_g \rightarrow 5b_{1u}$, $4b_{2g} \rightarrow 5b_{1u}$), two ligand-based $\pi \rightarrow \pi^*$ transitions ($3b_{3g} \rightarrow 5b_{1u}$, $3a_u \rightarrow 5b_{2g}$), and two $n \rightarrow \pi^*$ transitions ($15b_{3u} \rightarrow 5b_{2g}$, $16a_g \rightarrow 5b_{1u}$). In analogy to the ligand spectrum (Table I) the two ligand-based $n \rightarrow \pi^*$ transitions in the complex are expected to be very weak and the two ligand-based

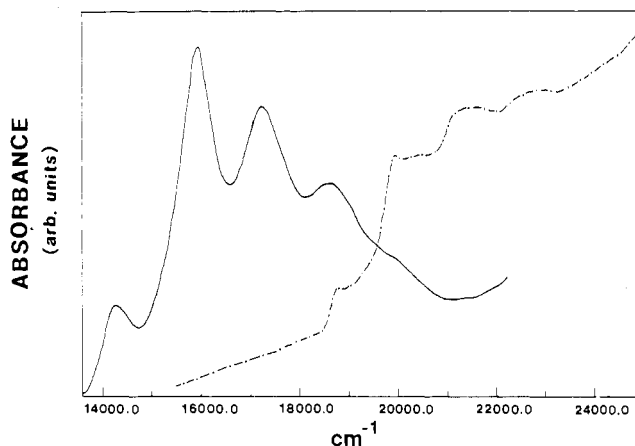


Figure 5. Comparative UV-vis spectra for (a) $Ni(N,N'-Bzl_2dto)_2Br_2$ (—) and (b) $N,N'-Bzl_2dto$ (---) in KBr pellets at 100 K ($N,N'-Bzl_2dto$ = N,N' -dibenzylidithiooxamide).

$\pi \rightarrow \pi^*$ transitions are expected to be very strong. In Figure 3a the UV band at 315 nm is perturbed only slightly from the energy of the $\pi \rightarrow \pi^*$ band in the free ligand (308 nm) and is of comparable intensity with respective molar absorptivities of 5.0×10^4 and $1.1 \times 10^4 M^{-1} cm^{-1}$. This observation, in conjunction with the molecular orbital analysis, strongly suggests that the band is predominantly a ligand-based $\pi \rightarrow \pi^*$ transition rather than a $L \sigma \rightarrow M$ charge-transfer transition as previously suggested.^{21c} The two symmetry-allowed valence $L \pi \rightarrow L \pi^*$ transitions both result in $^1B_{2u}$ excited states, even though the two transitions involve different orbitals ($3a_u \rightarrow 5b_{2g}$ and $3b_{3g} \rightarrow 5b_{1u}$). If it is assumed that relaxation effects are comparable for both of these transitions, our calculations predict that they occur at nearly the same energy and hence overlap to give the single observed band at 315 nm (Figure 3a). The two $n \rightarrow \pi^*$ transitions are predicted to occur at slightly higher energy than the two $L \pi \rightarrow L \pi^*$ transitions discussed above. The lower energy $15b_{3u} \rightarrow 5b_{2g}$ transition is predicted to occur in the same energy range as the two $L \pi \rightarrow L \pi^*$ transitions and, given its expected low intensity, would *prima facie* be overwhelmed by the intense $L \pi \rightarrow L \pi^*$ band. The energy necessary for the $16a_g \rightarrow 5b_{1u}$ transition is much greater than that for the $15b_{3u} \rightarrow 5b_{2g}$ transition. Hence, it is probable that this transition lies outside the spectral range accessible in the KBr matrix.

A comparison of the 298 K crystal spectrum of $N,N'-Bzl_2dto$ (Figure 2a) with the 298 K KBr spectrum of $Ni(N,N'-Bzl_2dto)_2Br_2$ (Figure 3b) shows that the pattern and energetic spacing of the bands are very similar and prompted us to investigate the low-temperature spectrum of $Ni(N,N'-Bzl_2dto)_2Br_2$. As shown in Figure 5a, the 100 K spectrum shows four well-defined peaks with λ_{max} values of 704, 629, 582, and 552 nm and a shoulder at ca. 504 nm.³⁴ For comparison, Figure 5b shows a 100 K KBr spectrum of $N,N'-Bzl_2dto$. The similarity in the pattern and energetic spacings of the bands clearly suggest that the two spectra are related. Since the five observed bands in the visible region of the $M(LH_2)_2X_2$ complexes cannot be accounted for, based solely on symmetry-allowed $M(d) \rightarrow L \pi^*$ electronic transitions, vibrational coupling must be considered. We suggest that the $Ni(d) \rightarrow L \pi^*$ transitions dominate the visible spectrum, and superimposed on this electronic band is a vibrational progression very similar to that found for the free ligand $n \rightarrow \pi^*$ transition. Support can be marshaled for this proposal. The temperature dependence of the position and intensity of the bands in the visible spectrum of $Ni(N,N'-Bzl_2dto)_2Br_2$ (Figures 3b and 5a), as well as the similarity of the ligand and metal complex spectra (Figure 5), clearly suggests that vibrational coupling may be involved. Coupled vibrational frequencies are characteristic of the excited

(33) Alvarez, S.; Hoffmann, R.; Vicente, R. *J. Am. Chem. Soc.* **1985**, *107*, 6253-6277.

(34) The broadness of the bands in Figure 5a suggests that under more favorable conditions (e.g., crystals or lower temperatures) additional structure may be observable. Effort is currently under way to achieve this.

state of the molecule. The excited states of both the ligand $n \rightarrow \pi^*$ transition and the $M(LH_2)_2X_2 M(d) \rightarrow L \pi^*$ transitions are derived from the lowest unoccupied π^* orbital of the ligand. Therefore, the bonding interactions and percent character composition for the two excited states are qualitatively very similar.

This interpretation of the spectrum allows several observations to be explained. The initial weak band at 704 nm is a $M(d) \rightarrow L \pi^*$ transition rather than a $d \rightarrow d$ transition as previously advanced but exhibits a weak coupling to a vibrational mode resulting in a low intensity. The loss of this band in the solution spectrum (Figure 3a) can be explained with the assumption, in analogy to the free ligand, that this band gains most of its intensity by coupling to a lattice mode that would not exist in the solution spectrum. In addition, it has been reported^{21c} that in the solid-state KBr spectra for the $M(N,N'-Me_2dto)_2Br_2$ complexes ($M = Ni, Pd, Pt$) the relative intensities and energetic spacings of the absorption bands in the visible region were scarcely influenced by the central metal. This observation can be explained quite readily according to our interpretation of the spectral data, which states that the relative intensities and energetic spacings of these bands would not be dependent on the central metal but rather on the energy of the coupled vibrational frequencies and on the intensity pattern of their associated Franck-Condon progressions.

Summary

In agreement with the previous spectral assignment of dithiooxamides,²⁰ the UV-vis spectrum for dithiooxamide has been shown to consist of two bands. The first band is a weak broad $n \rightarrow \pi^*$ transition occurring in the visible region and is assigned as ${}^1A_u \leftarrow {}^1A_g$ ($13a_g \rightarrow 4a_u$). The second band is an intense broad $\pi \rightarrow \pi^*$ transition occurring in the UV region and is assigned as ${}^1B_u \leftarrow {}^1A_g$ ($3b_g \rightarrow 4a_u$). Symmetrical N,N' -dialkylation of the dto moiety has been shown to cause a blue shift and an increase

in the molar absorptivity value for both of the transitions. A red shift of the transitions was observed for N,N' -bis(trimethylsilyl)dithiooxamide.

The $n \rightarrow \pi^*$ transition of the dithiooxamides reported here exhibits heretofore unreported vibrational fine structure, which clearly resolves upon temperature reduction. A preliminary analysis of the spectral data of N,N' -Bzl₂dto indicates that at least three vibrational frequencies are contributing to the observed spectrum. The two lower energy frequencies of ca. 52 and ca. 180 cm^{-1} are tentatively assigned as crystal lattice modes, while the major vibrational progression with a frequency of ca. 1150 cm^{-1} appears to involve the C-C stretch.

The spectra for $Ni(N,N'$ -Bzl₂dto)₂Br₂, which is representative of the $M(LH_2)_2X_2$ complexes, have been shown to consist of a series of bands in the visible region of varying intensity and an intense broad band in the UV region. In contrast to the previous assignment,^{21c} the UV band is assigned as a $L \pi \rightarrow L \pi^*$ transition. In partial agreement with the previous assignments,^{21a,c} the bands in the visible region for the $M(LH_2)_2X_2$ complexes are assigned as $M(d) \rightarrow L \pi^*$ transitions. However, the weak low-energy bands are not $d \rightarrow d$ transitions as previously advanced but are $M(d) \rightarrow \pi^*$ transitions. The multiplicity of bands in the visible region is caused by the coupling of one or more vibrational modes to allowed $M(d) \rightarrow L \pi^*$ transitions. The major vibrational progression resolves upon temperature reduction and appears to be qualitatively very similar to the major vibrational progression observed for the $n \rightarrow \pi^*$ transition of the free ligand.

Acknowledgment is made to the 3M Corp. and to the Research Corp. for partial financial support of this work. M.R.G. is grateful to The Ohio State University Graduate School for his support as a Presidential Fellow. We thank Roger H. Cayton for assistance in obtaining the low-temperature spectra.

Notes

Contribution from the Department of Chemistry,
The University of North Carolina,
Chapel Hill, North Carolina 27514

Intervalence Transfer in the Dimer [(NH₃)₅Ru^{II}(4,4'-bpy)Ru^{III}(NH₃)₅]⁵⁺

Joseph T. Hupp and Thomas J. Meyer*

Received June 10, 1986

In the study of mixed-valence compounds, ligand-bridged dimers based on the [(NH₃)₅Ru^{III/II}] couple have played a central role.¹ Notable examples include the Creutz and Taube ion,² [(NH₃)₅Ru(pz)Ru(NH₃)₅]⁵⁺ (pz = pyrazine), where the question of localization vs. delocalization is a source of continuing debate,¹⁻³ and the analogous 4,4'-bipyridine-bridged dimer, [(NH₃)₅Ru^{II}(4,4'-bpy)Ru^{III}(NH₃)₅]⁵⁺, where the valences appear to be trapped and the properties are well-defined in terms of available theory.⁴

We have reinvestigated a particular property of the latter ion, the solvent dependence of the energy of its intervalence transfer (IT) or metal-metal charge-transfer (MMCT) absorption band. On the basis of the results of our study and in light of recent developments in the area, we conclude that (1) there is a con-

siderable contribution to the apparent IT band energy arising from the existence of multiple IT transitions, (2) application of dielectric continuum theory to the solvent dependence of the IT band energy is not quantitatively successful, and (3) solvent effects whose origins arise at the molecular level may play a role in dictating the observed absorption band energies.

According to Hush,⁵ the band energy (E_{op}) for intervalence transfer in a chemically symmetrical mixed-valence dimer where electronic coupling is energetically negligible is given by

$$E_{op} = \chi_i + \chi_s \quad (1)$$

where χ_i and χ_s are the intramolecular (inner coordination sphere) and solvent reorganization or trapping energies, respectively. From dielectric continuum theory, χ_s is given by⁵

$$\chi_s = e^2 \left(\frac{1}{r} - \frac{1}{d} \right) \left(\frac{1}{D_{op}} - \frac{1}{D_s} \right) \quad (2)$$

In eq 2, e is the unit electronic charge, r is the molecular radius of the redox sites, d is the separation distance between trapping sites, and D_{op} and D_s are the optical and static dielectric constants of the solvent. The result in eq 2 is based on the assumption that the redox sites can be treated as nonpenetrating spheres. The effect of solvent has also been treated on the basis of the electronic redistribution that occurs within an ellipse enclosing the ion.⁶ For the case of interest here, the two-sphere model would appear to

- (1) See, for example: (a) Creutz, C. *Prog. Inorg. Chem.* **1983**, *30*, 1. (b) Taube, H. *Ann. N.Y. Acad. Sci.* **1978**, *313*, 481.
- (2) Creutz, C.; Taube, H. *J. Am. Chem. Soc.* **1969**, *91*, 3988; **1973**, *95*, 1086.
- (3) Fuerholz, U.; Bürgi, H. B.; Wagner, F. E.; Stebler, A.; Ammeter, J. H.; Krausz, E.; Clark, R. J. H.; Stead, M.; Ludi, A. *J. Am. Chem. Soc.* **1984**, *106*, 121.
- (4) (a) Tom, G. M.; Creutz, C.; Taube, H. *J. Am. Chem. Soc.* **1974**, *96*, 7828. (b) Creutz, C. *Inorg. Chem.* **1978**, *17*, 3723.

- (5) Hush, N. S. *Prog. Inorg. Chem.* **1967**, *8*, 391.
- (6) (a) Brunschwig, B. S.; Ehrenson, S.; Sutin, N. *J. Phys. Chem.* **1986**, *90*, 3657. (b) Cannon, R. D. *Chem. Phys. Lett.* **1977**, *49*, 299. (c) Kharkats, Yu I. *Elektrokhimya* **1976**, *15*, 1251. (d) German, E. D. *Chem. Phys. Lett.* **1979**, *64*, 305.